



ELSEVIER

Available online at www.sciencedirect.com

SCIENCE @ DIRECT®

Journal of Magnetism and Magnetic Materials 288 (2005) 205–213



www.elsevier.com/locate/jmmm

Ferromagnetic resonance and magnetization studies in exchange-coupled NiFe/Cu/NiFe structures

L.C.C.M. Nagamine^{a,*}, J. Geshev^a, T. Menegotto^a, A.A.R. Fernandes^b,
A. Biondo^b, E.B. Saitovitch^c

^a*Instituto de Física, UFRGS, Av. Bento Gonçalves, 9500, C.P. 15051, 91501-970, Porto Alegre, RS, Brazil*

^b*Departamento de Física, UFES, 29060-900, Vitória, ES, Brazil*

^c*Centro Brasileiro de Pesquisas Físicas–CBPF, Rio de Janeiro, RJ, Brazil*

Received 18 June 2004; received in revised form 3 September 2004

Available online 5 October 2004

Abstract

We report on the dependence of the ferromagnetic resonance and magnetization on the NiFe thickness, t , of NiFe/Cu(9 Å) magnetic monolayers and symmetrical NiFe/Cu(9 Å)/NiFe/Cu(9 Å) exchange-coupled magnetic bilayer structures, deposited onto Si(1 0 0) substrate. The out-of-plane resonance field variations showed the presence of both the acoustic and optic precession modes in most of the bilayer structures. These variations and the magnetization curves were fitted using a phenomenological model, which indicated different effective magnetizations for the first and second NiFe layers as well as dependence of the magnetization and the coupling on t . Up to $t = 43$ Å, the bilayers are discontinuous and direct interaction between the adjacent NiFe layers occurs. For higher t , they could be considered continuous and the exchange coupling changes from ferromagnetic to antiferromagnetic at $64 \text{ Å} < t < 128 \text{ Å}$. Coexistence of ferromagnetic and antiferromagnetic coupling was detected for the bilayer with $t = 1280$ Å, for which a biquadratic interlayer exchange coupling was also considered in the fittings, indicating the presence of pinholes. The results show that the techniques used are very sensitive for the evaluation of the continuity of the layers, the exchange coupling, and the possible presence of pinholes in such structures.

© 2004 Elsevier B.V. All rights reserved.

PACS: 76.50.+g; 75.70.Ak; 75.30.Gw

Keywords: Ferromagnetic resonance; Magnetic properties of monolayers and thin films; Magnetic anisotropy

*Corresponding author. Tel.: 555133166543; fax: 555133167286.

E-mail address: nagamine@if.ufrgs.br (L.C.C.M. Nagamine).

1. Introduction

The interlayer exchange coupling between ferromagnetic (FM) layers mediated by nonmagnetic spacer plays a key role for understanding of many properties observed in magnetic/non-magnetic artificial structures. One example is the giant magnetoresistance effect which is related to the antiferromagnetic (AF) coupling between adjacent magnetic layers [1]. Artificial structures containing magnetically soft Permalloy are potential candidates for magnetic recording devices such as magnetoresistive read heads and nonvolatile random access memories.

Ferromagnetic resonance (FMR) is a powerful technique for understanding the nature and the extent of exchange interactions in magnetic thin films and multilayers (see Ref. [2] and the references therein). The resonance modes depend on the intralayer as well on the interlayer magnetic coupling. In order to apply this technique, however, one must be able to obtain the equilibrium positions of the magnetization vectors which, in general, is very difficult to be done when the energy expression involves terms different from the uniaxial anisotropy ones. Dispersion relation expressions for trilayer [3–5] and multilayer structures [6,7] have been derived by several groups. Although a lot of work has been done applying the FMR technique for investigation of trilayer systems [2,8], there still remain open questions, mainly related to the uniaxial anisotropy of each layer. Lindner et al. [9] studied in situ the FMR phenomenon for Ni/Cu/Co(001) structures, where the in-plane precession modes were studied as a function of temperature. Detailed study of the out-of-plane FMR variations for such structures, however, is still lacking. Even when these modes are investigated, as is the case of NiFe/Cu/NiFe trilayer structures [10,11], their interpretation is only qualitative and incomplete.

In the present work FMR and magnetization measurements have been performed on NiFe magnetic monolayer (capped with 9 Å Cu layer), and NiFe/Cu/NiFe/Cu magnetic bilayer structures, i.e., separated and capped with Cu layers, varying the NiFe (here, Ni₈₁Fe₁₉) thickness, t , in

the range from 21 to 1280 Å. The Cu layer thickness of 9 Å was chosen as to correspond to the first peak of the AF coupling, which has been precisely determined from magnetoresistance measurements [12], where magnetoresistance amplitude of 22% was obtained for Fe(90 Å)/Cu(9 Å)/[(NiFe(16 Å)/Cu(9 Å))₂₀ sample grown in the same conditions.

2. Experiment

The NiFe(t)/Cu(9 Å) and NiFe(t)/Cu(9 Å)/NiFe(t)/Cu(9 Å) structures were prepared by magnetron sputtering in 2.0 mTorr Ar atmosphere, where NiFe was grown by RF sputtering at deposition rate of 1.0 Å/s and Cu by DC sputtering at 1.2 Å/s. NiFe was chosen to be RF sputtered in virtue of its enhanced structural quality as compared to be DC sputtered, as shown by Cowache et al. [13]. The deposition rates and film thicknesses were obtained by low-angle X-ray analysis. The base pressure was better than 5×10^{-8} Torr and the substrate was a Si(100) with a native SiO₂ layer. The structural characterization was made via conventional X-ray powder diffraction performed on a Philips X'Pert MRD machine employing Cu $K\alpha$ radiation. Both NiFe and Cu layers were polycrystalline, with no indication of dominant textured structure.

Room temperature magnetization data were obtained using a home-made alternate gradient force magnetometer with sensibility of about 10^{-7} emu, where the external magnetic field was applied in the film's plane. A superconducting quantum interference device (SQUID) magnetometer was also used to precisely estimate the saturation magnetization.

FMR measurements were performed at room temperature using a Varian X-band (9.5 GHz) electron spin resonance spectrometer with a rectangular TE₁₀₂ microwave cavity, with standard phase-sensitive detection technique. The samples were mounted on the tip of an external goniometer to allow measurements of the resonance field as a function of the in-plane (ϕ_H) or out-of-plane (θ_H) angles.

3. Model

Recently, a phenomenological model has been developed by some members of our group which allows to obtain the dispersion relation for any exchange coupling strength and for any magnetic field, even if the system is unsaturated at resonance. The model has been applied to exchange-biased uniaxial FM/AF bilayers assuming formation of planar domain wall at the AF side of the interface for various exchange field strengths and for both cases of FM and AF coupling [14,15], as well as to exchange-coupled systems characterized by competing uniaxial and cubic anisotropies [16]. In the present work, the model was applied on a system that consists of two magnetic layers, denoted as A and B, with saturation magnetizations M_s^A and M_s^B and thicknesses t_A and t_B , respectively, exchange-coupled through a nonmagnetic layer. The anisotropic part of the total free energy of this system per unit area can be written as

$$E = t_A E_A + t_B E_B + E_{\text{int}}. \quad (1)$$

The energies involved in E_k (where $k = A$ or B),

$$E_k = -\mathbf{H} \cdot \mathbf{M}_s^k + 2\pi(\mathbf{M}_s^k \cdot \mathbf{n})^2 - K_U^k (\mathbf{M}_s^k \cdot \mathbf{n}/M_s^k)^2 \quad (2)$$

are the corresponding Zeeman energy (the first term), the demagnetizing energy (the second term), and the last term corresponds to the uniaxial anisotropy energy. It is assumed here (in accordance with the experimental data) that both magnetic layers show perpendicular-to-the-plane uniaxial anisotropy only; \mathbf{n} is a unit vector normal to the film's plane, and K_U^k is the k th uniaxial anisotropy constant. In thin films, the K_U^k values depend on the interface-induced anisotropy, stress-induced anisotropy, and volume magneto-crystalline anisotropy of each magnetic layer. The last term in Eq. (1) is the bilinear exchange coupling energy,

$$E_{\text{int}} = -J_1 \mathbf{M}_s^A \cdot \mathbf{M}_s^B / (M_s^A M_s^B), \quad (3)$$

with J_1 being the interlayer exchange coupling constant; $J_1 > 0$ and $J_1 < 0$ correspond to FM and AF coupling, respectively.

The first derivatives of E with respect to the polar (θ_k) and azimuthal (ϕ_k) angles of \mathbf{M}_s^k in spherical coordinates must be equal to zero at equilibrium. Each vector \mathbf{M}_s^k , if perturbed from its equilibrium orientation, will precess around its equilibrium direction. Following Smit and Beljers [17], the roots of the determinant of the 4×4 matrix

$$\begin{bmatrix} E_{\theta_A \theta_A} & E_{\theta_A \phi_A} + iz_A & E_{\theta_A \theta_B} & E_{\theta_A \phi_B} \\ E_{\theta_A \phi_A} - iz_A & E_{\phi_A \phi_A} & E_{\theta_B \phi_A} & E_{\phi_A \phi_B} \\ E_{\theta_A \theta_B} & E_{\theta_B \phi_A} & E_{\theta_B \theta_B} & E_{\theta_B \phi_B} + iz_B \\ E_{\theta_A \phi_B} & E_{\phi_A \phi_B} & E_{\theta_B \phi_B} - iz_B & E_{\phi_B \phi_B} \end{bmatrix}$$

will give the dispersion relation of the exchange-coupled system, i.e., a fourth-order equation in ω (the angular frequency of precession) with at most two meaningful solutions (precession modes) at any given DC field. Here E_{kl} 's ($k, l = A$ or B) denote the second derivatives with respect to the equilibrium angles θ_k^0 and ϕ_k^0 of the energy given in Eq. (1), $z_k = (\omega/\gamma_k)t_k M_s^k \sin \theta_k^0$, and γ_k is the gyromagnetic ratio of the k th layer, with $\gamma_k = 2\pi g \mu_B/h$; where g , μ_B and h are the g -factor, Bohr magneton number, and the Planck constant, respectively. One of the precession modes is characterized by an in-phase precession and is normally called 'acoustic' mode, while the other one consists of out-of-phase spin oscillations and is classified as 'optic'.

When the magnetic layers are of the same material (in this work, NiFe), if they have equal thicknesses (symmetrical structures), and are weakly coupled, and also if the DC field is larger than the saturation field, then the acoustic mode is degenerated with that of the uncoupled case and the optic mode is shifted [2] by a magnetic field value of $\pm 2J_1/(M_s t)$ in the case of NiFe, where the positive sign is for AF coupling and the negative sign is for FM coupling. The intensity of the optic mode is weaker than the acoustic one and depends on the ratio between the difference of the uniaxial anisotropy of the two NiFe layers and the exchange-coupling field [2]. Moreover, the optic mode is much easier to be observed when the applied magnetic field is perpendicular to the film than parallel to it. If the two NiFe layers have the same uniaxial anisotropy, the intensity of the optic

mode will be zero. Hence, both the type and intensity of the coupling can be achieved through the identification of the two modes and from the difference between their resonance fields, when the external field is in the film's plane. The uniaxial anisotropy of the two NiFe layers can be obtained from the fit of the angular variations of the resonance fields using the model described above, since M_s is known.

4. Results and discussion

The in-plane resonance field and the magnetization data do not vary significantly from one sample to another, which is in agreement with the X-ray results for both monolayer and bilayer samples, showing no indications for dominant texture structure, neither for NiFe nor for Cu crystallites. The maximum difference between the lowest and highest resonance field values was found to be 10 Oe, which can be considered as negligible. Thus, these data are not presented here.

The experimental out-of-plane resonance field data for the monolayer samples with $t \geq 35 \text{ \AA}$, i.e., Si(1 0 0)/SiO₂/NiFe(t)/Cu(9 \text{ \AA}), are shown in Fig. 1 along with the corresponding fitting curves. It was impossible to obtain reasonable resonance field signal for the monolayer with $t = 21 \text{ \AA}$, which can be ascribed to a non-homogeneous and probably discontinuous magnetic layer at this thickness. The effective magnetizations, M_{eff} , for the NiFe layers [where $4\pi M_{\text{eff}} = 4\pi M_s - H_U$ for $H_U = 2K_U/(M_s t)$] given in Table 1 were evaluated from the out-of-plane FMR data in the framework of the model described above; the numerical procedure used has been published elsewhere [14–16]. As can be seen in the figure, the estimated resonance field angular variations agree very well with the experimental data. The linewidth of the resonance signal for $t = 128 \text{ \AA}$ was $\approx 50 \text{ Oe}$ for parallel configuration and $\approx 70 \text{ Oe}$ for perpendicular configuration. The resulting from both monolayer and bilayer series fitting values for $\gamma/2\pi$ are 2.92 GHz/kOe (i.e., $g = 2.09$) for samples with $t = 21 \text{ \AA}$ and 35 \AA , and 2.94 GHz/kOe (i.e., $g = 2.10$) for the others, the latter value

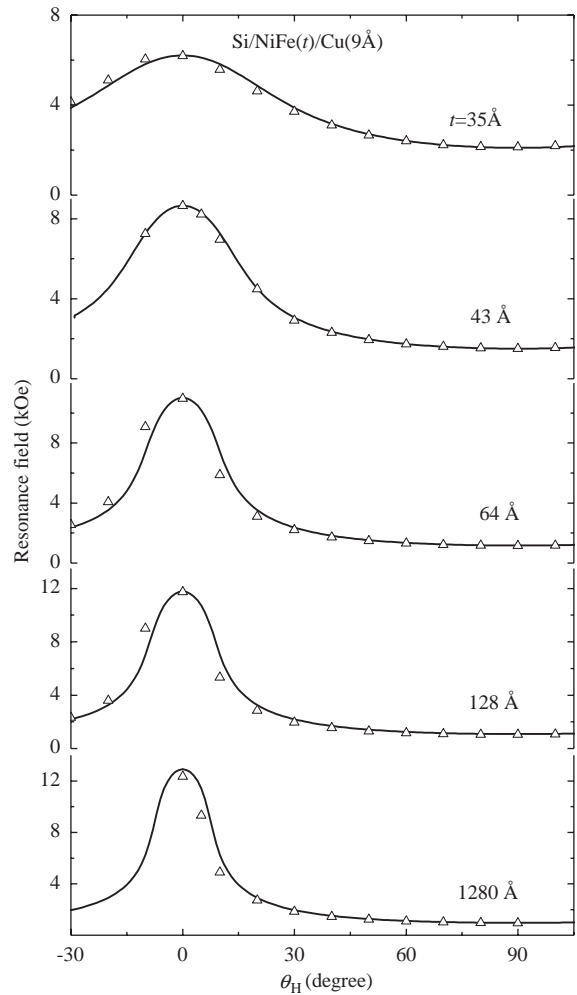


Fig. 1. Room temperature angular variations of the resonance field for NiFe(t)/Cu(9 \text{ \AA}) series. The symbols represent the experimental data and the curves are the corresponding fittings using the parameters given in Table 1.

being typical for bulk NiFe [18]. The saturation magnetization was obtained through SQUID measurements of the bilayer samples assuming that the two FM layers have one and the same saturation magnetization. These results are shown in Table 1.

FMR spectra for some of the bilayer samples for static magnetic field parallel (H_{\parallel}) and perpendicular (H_{\perp}) to the film's plane are shown in Fig. 2. The spectra are the field derivative of the absorbed

Table 1

Parameters deduced from the fittings of the fourlayer structures with composition Si/SiO₂/NiFe(1)(*t*)/Cu(9 Å)/NiFe(2)(*t*)/Cu(9 Å), where the values for the effective magnetization, $4\pi M_{\text{eff}}^{(1)}$ given in parentheses are the results obtained for the Si/SiO₂/NiFe(*t*)/Cu(9 Å) monolayer series

<i>t</i> (Å)	J_1 (10 ⁻² erg/cm ²)	$4\pi M_s$ (kOe)	$4\pi M_{\text{eff}}^{(1)}$ (kOe)	$4\pi M_{\text{eff}}^{(2)}$ (kOe)
21	0.1	6.81	4.25	4.25
35	0.1	7.16	5.48 (2.95)	5.48
43	0.2	7.41	7.40 (5.43)	7.00
64	1.4	9.17	7.78 (7.78)	8.70
128	-1.3	9.55	8.55 (8.55)	9.30
1280	-2.0	9.80	9.78 (9.78)	9.80

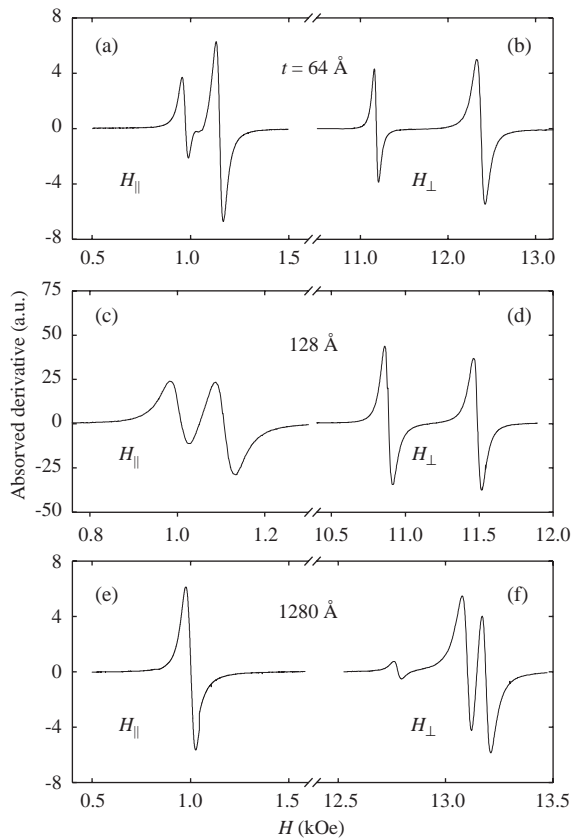


Fig. 2. In-plane [panels (a), (c) and (e)] and out-of-plane [panels (b), (d) and (f)] FMR spectra at 9.5 GHz for NiFe(*t*)/Cu(9 Å) and NiFe(*t*)/Cu(9 Å)/NiFe(*t*)/Cu(9 Å) series at room temperature.

power. For $t = 64 \text{ \AA}$ (the upper panel of this figure), the resonance has a relatively intense optic mode on the low field side of the main mode, indicating a weak FM coupling between the NiFe layers. The intensities of the two modes are almost equal for $t = 128 \text{ \AA}$ (Fig. 2c) when the field is applied in the film's plane. In the perpendicular configuration, however, it is clear that the optic peak is located at a higher field than the main mode, indicating a weak AF interlayer exchange coupling for this sample.

The spectrum for $t = 1280 \text{ \AA}$ with the field applied perpendicular to the plane (Fig. 2f) shows three resonance peaks. The strongest intermediate peak is the main mode. The peak located at the higher field side is the optic one. The resonance peak corresponding to the optic mode is observed at higher field than the main mode, indicating an AF interlayer exchange coupling. However, for this sample, in addition to the bilinear exchange coupling [Eq. (3)], a biquadratic coupling term, $J_2 [\mathbf{M}_s^A \cdot \mathbf{M}_s^B / (M_s^A M_s^B)]^2$, was included in the model (where J_2 is the corresponding coupling constant), which favors orthogonal magnetizations alignment. The peak on the low field side is rather weak at the perpendicular configuration and is identified as being due to a higher order volume spin-wave mode [19,20]. Such a mode, located at 12.15 kOe, is also detected in the perpendicular configuration for the monolayer with $t = 1280 \text{ \AA}$, while the main mode is located at 12.35 kOe. This mode has also been observed for poly- and mono-crystalline NiFe monolayers by Schmool et al. [21]. The biquadratic coupling term will be discussed in more details later in this paper.

The out-of-plane angular variations of the resonance field for the bilayer series are shown in Fig. 3. One notes that for $t = 21$ and 35 \AA there is one precession mode only. The interlayer exchange coupling strength for the bilayer series and the best fit of the effective magnetization for NiFe(1) and NiFe(2) layers [here (1) and (2) denote the first and the second NiFe layers, respectively] are also displayed in Table 1. They were evaluated from the fitting of both the out-of-plane FMR data as well as from the magnetization curves (see Fig. 4) for the bilayer samples.

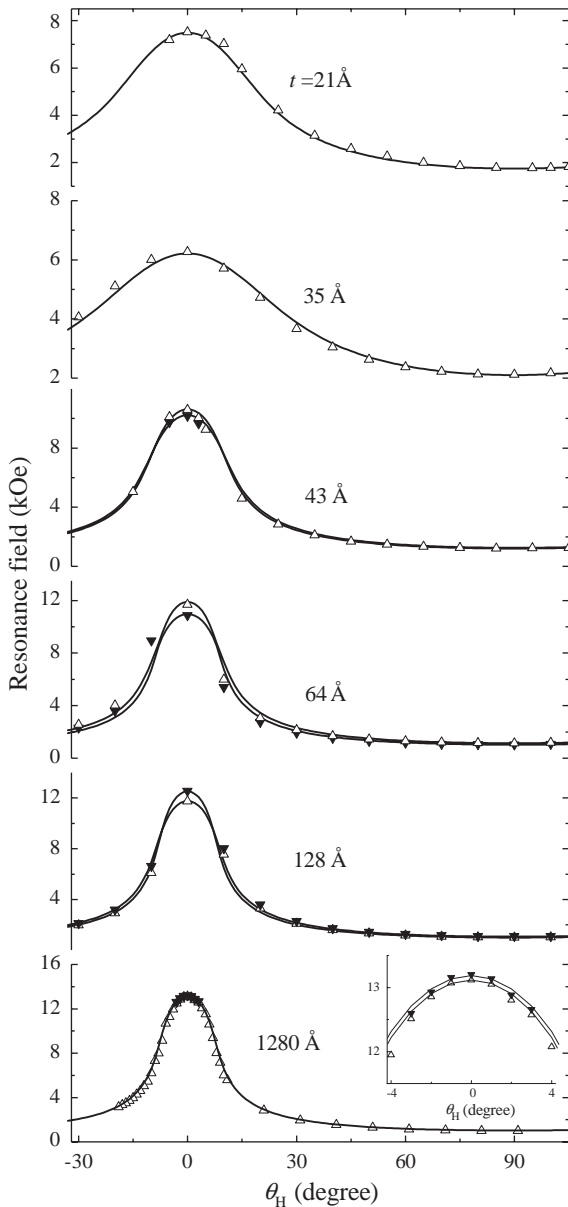


Fig. 3. Angular variation of the resonance field for the NiFe(t)/Cu(9 Å)/NiFe(t)/Cu(9 Å) series at room temperature. Open triangles represent the acoustic (in-phase) mode and full triangles represent the optic (out-of-phase) mode of precession, and the solid and dashed lines are the corresponding best fitting curves. The inset shown in the bottom panel is a zoom of the $-4^\circ \leq \theta_H \leq 4^\circ$ region.

The existence of only one precession mode for $t = 21$ and 35 Å could be attributed to approximately equal uniaxial anisotropy constants of the

two NiFe layers. In this case, the resonance field of the acoustic mode should coincide with that of the NiFe monolayer, since this mode is degenerated for an uncoupled system [2]. Distinct values for these resonance fields, however, were obtained from the FMR data fits (see the fourth column in Table 1), indicating that the NiFe layers are discontinuous for these bilayers. For $t = 43$ Å, another peak appears on the low field side of the main peak at the perpendicular configuration (optic mode) in the FMR spectra. Nonetheless, this sample should not be completely continuous since large difference between the effective magnetizations is obtained by comparing this bilayer with the corresponding monolayer. The presence of only one mode for $t = 1280$ Å in the parallel configuration is attributed here to approximately the same anisotropy constant value of the NiFe(1) and NiFe(2) layers. The inset shown in the bottom

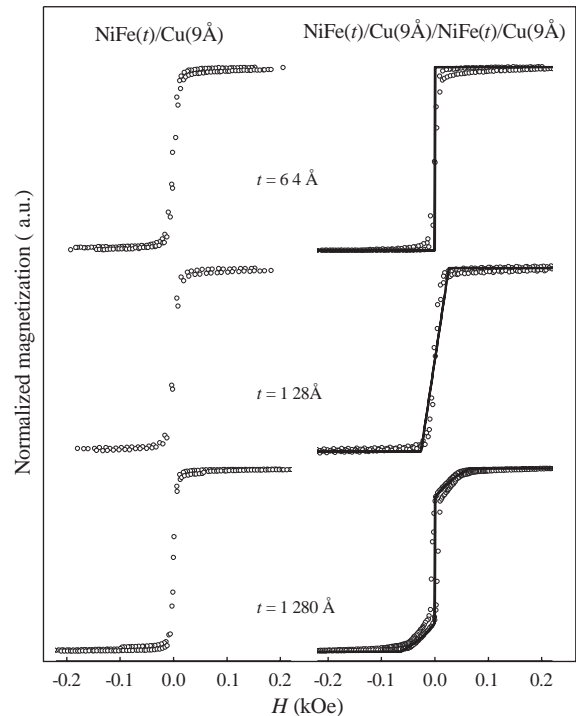


Fig. 4. Normalized to M_s room temperature in-plane hysteresis loops for the NiFe(t)/Cu(9 Å) and NiFe(t)/Cu(9 Å)/NiFe(t)/Cu(9 Å) series with $t = 64$, 128 and 1280 Å, where the symbols and lines represent the experimental and fitted curves, respectively.

panel in Fig. 3 represents the experimental data and the fittings for $-4^\circ \leq \theta_H \leq 4^\circ$ where, in this case, the biquadratic term has been included in the calculations with $J_2 = 0.15$ erg/cm², the latter being rather higher than the corresponding absolute value of J_1 (i.e., 0.02 erg/cm², see Table 1). The agreement between the experimental data and the fittings seems to be quite good.

In-plane magnetic hysteresis loops for some of the monolayer and bilayer samples are plotted in Fig. 4. A normalized to M_s remanent magnetization of 0.68 and a saturation field of 70 Oe were obtained for the bilayer with $t = 1280$ Å, indicating coexistence of ferromagnetic and antiferromagnetic couplings for this sample. A biquadratic term was initially used by Rührig et al. [22] to fit the magnetization curves of their exchange-coupled multilayers; it has also been taken into account by other authors [23,24]. Bobo et al. [25] showed that the physical process that produces these magnetization curves is, in fact, pinhole coupling. In the present work, the agreement between the fitted and experimental hysteresis loops is rather good (see Fig. 4), despite the fact that the phenomenological model used here considers coherent magnetization rotation only, discarding possible domain wall nucleation and motion.

The coupling between the NiFe layers at this copper thickness can be due to two factors, essentially. One is the fluctuation of the bilinear coupling [26,27] due to the small variations of the distance between the NiFe layers through the Cu. This could be provoked by the intermixing between NiFe and Cu at the interfaces, the latter being paramagnetic [12]. The other factor could be presence of pinholes that are able to couple directly the two magnetic layers. The high orthogonal coupling constant, obtained for $t = 1280$ Å as compared with the J_1 value for $t = 64$ Å, indicates that for the former sample the magnetic behavior is determined by pinholes and by fluctuation of the bilinear coupling for the latter sample.

The deduced J_1 values (-0.013 and -0.020 erg/cm²) obtained for the bilayers with $t = 128$ and 1280 Å, respectively, are in agreement with the previously reported by Parkin et al. [28]

(-0.020 erg/cm²) and Nagamine et al. [12] (-0.018 erg/cm²) for NiFe/Cu multilayers.

The effective magnetizations for NiFe(1) and NiFe(2) layers as a function of $1/t$ for the continuous bilayers (i.e., $t \geq 64$ Å) are given in Fig. 5. They can be fitted with the help of the frequently used expression [29]

$$4\pi M_{\text{eff}}(t) = 4\pi M_{\text{eff}}(\infty) \left(1 - \frac{2\Delta d}{t}\right), \quad (4)$$

which reflects the reduction of the NiFe magnetization at both types of interfaces, i.e., SiO₂/NiFe(1) and NiFe(1)/Cu interfaces, and Cu/NiFe(2) and NiFe(2)/Cu interfaces (Δd is the interfacial non-magnetic layer thickness). The linear fits gave $4\pi M_{\text{eff}}$ bulk values of (9.80 ± 0.10) kOe for NiFe(1) and (9.85 ± 0.10) kOe for the NiFe(2) layers. These values are consistent with the ones obtained for Cu/NiFe/Cu structures [30] (≈ 9.8 kOe). Assuming that $2\Delta d$ corresponds to the nonmagnetic layers in SiO₂/NiFe(1) and NiFe(1)/Cu, or Cu/NiFe(2) and NiFe(2)/Cu interfaces, one also obtains a total of (14.0 ± 2.0) Å and (7.4 ± 0.5) Å for $2\Delta d$, respectively. By considering each NiFe/Cu and Cu/NiFe interfaces as (3.7 ± 0.3) Å thick, existence of magnetically inactive layer of (10.3 ± 1.6) Å can be deduced for the SiO₂/NiFe interfaces.

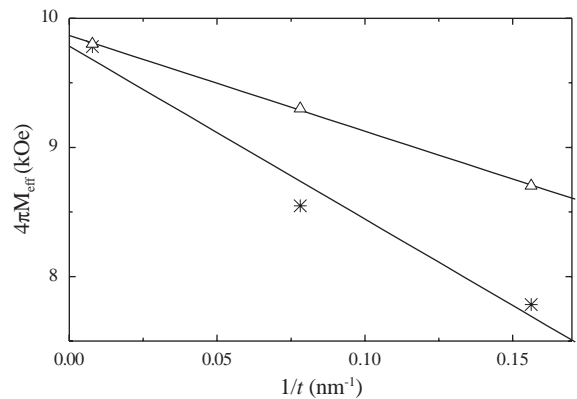


Fig. 5. The effective magnetization as a function of $1/t$. The open circles are the experimental results for the first NiFe layer, NiFe(1), and the asterisks are for the second one, NiFe(2), for the bilayer structure with the composition Si/SiO₂/NiFe(1)(t)/Cu(9 Å)/NiFe(2)(t)/Cu(9 Å). The lines are linear fits to the experimental data.

Studies on NiFe/Cu multilayers [12,31] showed that a 54 Å thick NiFe buffer layer is necessary in order to obtain strong AF coupling in such systems, where magnetically inactive layers of (3 ± 1) Å at each interface were obtained by conversion electron Mössbauer spectroscopy. Therefore, our estimation for the non-magnetic interfacial layer thickness for the bilayer samples is in good agreement with those obtained for NiFe/Cu multilayers. The different values obtained for $4\pi M_{\text{eff}}$ for NiFe(1) and NiFe(2) could be attributed to the interface-induced or stress-induced anisotropy, since the first layer is grown directly on the Si substrate, and the second layer is grown on the NiFe/Cu structure.

In summary, the magnetic characteristics of symmetrical NiFe/Cu(9 Å)/NiFe/Cu(9 Å) structures were studied by using magnetization and FMR experiments, when the NiFe layers' thickness was varied. It was shown that, in order to obtain AF coupling for such films with 9 Å thick Cu spacer, the NiFe thickness is necessary to be, at least, higher than 64 Å. For the sample with $t = 1280$ Å, coexistence of FM and AF couplings was found. The effective normal-to-the-plane uniaxial anisotropies were estimated for the first and second NiFe layers for the bilayer structures. Magnetically inactive layer of (3.7 ± 0.3) Å was estimated for the NiFe/Cu and Cu/NiFe interfaces and of about (10.3 ± 1.6) Å for the SiO₂/NiFe interfaces from the variation of the effective magnetization as a function of the NiFe thickness. The difference between the effective magnetization values of the NiFe layers is attributed to the interface-induced or stress-induced anisotropies. The results demonstrate that the combination of the two techniques used here for the characterization of the samples is very successful for the evaluation of the continuity of the layers, the exchange coupling, as well as possible presence of pinholes in such structures.

Acknowledgements

The authors wish to thank V.C. Santos for assistance with the FMR measurements. This work has been supported by the Brazilian agencies

CNPq, FAPERGS, and FAPERJ (Cientista do Nosso Estado).

References

- [1] M.N. Baibich, J.M. Broto, A. Fert, F. Nguyen Van Dau, F. Petroff, P. Etienne, G. Creuzet, A. Friederich, J. Chazelas, Phys. Rev. Lett. 61 (1988) 2472.
- [2] Z. Zhang, L. Zhou, P.E. Wigen, K. Ounadjela, Phys. Rev. B 50 (1994) 6094.
- [3] M. Vohl, J. Barnas, P. Grunberg, Phys. Rev. B 39 (1989) 12003.
- [4] B. Heinrich, S.T. Purcell, J.R. Dutcher, K.B. Urquhart, J.F. Cochran, A.S. Arrot, Phys. Rev. B 38 (1988) 12879.
- [5] A. Layadi, J. Appl. Phys. 83 (1998) 3738.
- [6] J.J. Krebs, P. Lubitz, A. Chaiken, G.A. Prinz, Phys. Rev. Lett. 63 (1989) 1645.
- [7] G.V. Sudhakar Rao, A.K. Bhatnagar, F.S. Razavi, J. Magn. Magn. Mater. 247 (2002) 159.
- [8] S.M. Rezende, C. Chesman, M.A. Lucena, A. Azevedo, F.M. de Aguiar, S.S.P. Parkin, J. Appl. Phys. 84 (1998) 958.
- [9] J. Lindner, Z. Kollonitsch, E. Kosubek, M. Farle, K. Baberschke, Phys. Rev. B 63 (2001) 094413.
- [10] S.M. Zhou, et al., Phys. Stat. Sol. 181 (1994) K65.
- [11] S. Ishio, H. Koizumi, H. Kubota, Y. Ando, T. Miyazaki, Phys. Stat. Sol. 139 (1993) K125.
- [12] L.C.C.M. Nagamine, A. Biondo, L.G. Pereira, A. Mello, J.E. Schmidt, T.W. Chimendes, J.B.M. Cunha, E.B. Saitovitch, J. Appl. Phys. 94 (2003) 8979.
- [13] C. Cowache, et al., Phys. Rev. B 53 (1996) 15027.
- [14] J. Geshev, L.G. Pereira, J.E. Schmidt, Phys. Rev. B 64 (2001) 184411.
- [15] J. Geshev, L.G. Pereira, J.E. Schmidt, L.C.C.M. Nagamine, E.B. Saitovitch, F. Pelegrini, Phys. Rev. B 67 (2003) 132401.
- [16] J. Geshev, L.G. Pereira, J.E. Schmidt, Physica B 320 (2002) 169.
- [17] J. Smit, H.G. Beljers, Philips Res. Rep. 10 (1955) 113.
- [18] C.E. Patton, Z. Frait, C.H. Wilts, J. Appl. Phys. 46 (1975) 5002.
- [19] A.Z. Maksymowicz, J.S.S. Whiting, M.L. Watson, A. Chambers, Thin Solid Films 197 (1991) 287.
- [20] H. Puszkarski, Prog. Surf. Sci. 9 (1979) 191.
- [21] D.S. Schmool, J.S.S. Whiting, A. Chambers, E.A. Wilinska, J. Magn. Magn. Mater. 131 (1994) 385.
- [22] M. Rührig, R. Schäffer, A. Hubert, R. Mosler, J.A. Wolf, S. Demokritov, P. Grünberg, Phys. Status Solidi A 125 (1991) 635.
- [23] B. Rodmacq, K. Dumesnil, Ph. Mangin, M. Hennon, Phys. Rev. B 48 (1993) 3556.
- [24] J.J. Krebs, G.A. Prinz, M.E. Filipkowski, C.J. Gutierrez, J. Appl. Phys. 79 (1996) 4525.
- [25] J.F. Bobo, H. Kikuchi, O. Redon, E. Snoeck, M. Picuch, R.L. White, Phys. Rev. B 60 (1999) 4131.

- [26] J.C. Slonczewski, *Phys. Rev. Lett.* 67 (1991) 3172.
- [27] J.C. Slonczewski, *J. Appl. Phys.* 73 (1993) 5957.
- [28] S.S.P. Parkin, *Appl. Phys. Lett.* 61 (1992) 1358.
- [29] J. Dubowik, F. Stobiecki, T. Lucinski, *Phys. Rev. B* 57 (1998) 5955.
- [30] S. Mizukami, Y. Ando, T. Miyazaki, *Jpn. J. Appl. Phys.* 40 (2001) 580.
- [31] L.C.C.M. Nagamine, A. Biondo, L.G. Pereira, A.F. Souza, A. Mello, J.E. Schmidt, M.B. Fontes, E. Baggio-Saitovitch, *J. Magn. Magn. Mater.* 242–245 (2002) 541.